

Influence of Ti-Ceramic or Ti-Composite crown on stress distribution: finite element study and additive manufacturing

A. ISPAS^{a*}, C. COSMA^b, A. CRACIUN^a, M. CONSTANTINIUC^a, L. LASCU^a, D. LEORDEAN^b, C. VILAU^b

^a *Department of Prosthodontics, "Iuliu Hatieganu" University of Medicine and Pharmacy, Cluj-Napoca, Romania*

^b *Technical Univesity of Cluj-Napoca, Romania*

The purpose of this study was to evaluate the tension distribution induced in teeth and dental prostheses, using the finite element method (FEA). Mathematical models, with the highest fidelity degree in representing the anatomical dimensions of the tooth and Ti-Ceramic, respectively Ti-Composite crowns were constructed using the finite element method. The models were built from a patient CBCT (cone beam computed tomography). There were six different scenarios of occlusal strain developed, among which two of them were placed on the contact points. The other four were distributed in a single point with vertical, respectively oblique direction. The applied force values were 67N, 135N and 454N. The FEA analysis demonstrates that the composite material undertakes and transfers all the tensions to the Ti substructure, which leads to slightly higher tension in dentine compared with the natural premolar. The Ti-Ceramic crown absorbs some of the tension and distributes to the dentine approximately the same tension as the enamel of the natural premolar.

(Received July 12, 2016; accepted September 29, 2016)

Keywords: Titanium, Ceramic, Composite, von Mises equivalent stress, Occlusal trauma, Selective laser melting

1. Introduction

Researchers examined the effects of biomechanical occlusal loads which act on the teeth during mastication [1, 2, 3]. Because of functional reasons, the internal and external architecture of the tooth causes the increased distribution of the tension generated by the mastication forces both in the tooth and in the supporting structures and alveolar bone [4].

The pattern of tension distribution in the tooth and in its supporting tissues is influenced by the implantation of tooth, its position, the intensity and direction of the forces. Determining the nature and direction of the forces dispersed in the periodontal ligament is a critical element for a better understanding of the biological behavior of the supporting structure of the tooth, in good functional condition or occlusal trauma [3, 5].

In order to accurately assess the selective forces acting on these tooth tissues, it is important to understand the structural and functional characteristics of the mastication system. Understanding this process involves defining the type of occlusal forces resulting from the masticatory system [6].

Hojjatie et al.[7] Palamara and collaborators[8] have studied the influence of occlusal forces on dentin and restoration using Finite Element Analysis (FEA), while Kamposiora [9] and collaborators have studied the specific effect of the cement layer on the restoration, taking into account the occlusal forces. Proos and collaborators [10, 11, 12, 13] have insisted on the marginal design, on various luting materials, on the design of the cement layer, types of cores used and the thickness of the restoration.

Based on these studies, it was hypothesized that FEA studies constitute an appropriate means to assess dental restorations or customized medical implants [14, 15]. These simulations prevent the destruction of specimens and enable the testing of different materials for prosthetic restoration [16]. FEA studies have a fundamental importance in gaining knowledge of the mechanism by which these elements relate in terms of functionality to optimize clinical outcomes [17].

Therapy in fixed dental prosthetics makes use of a wide range of dental materials. Although metals are often responsible for allergies, they are most commonly used. In these situations, the recommendation would be to replace the CoCr substructure with one from Titanium (Ti). Thus, the substructure of the dental crowns will provide resistance to enhanced corrosion, greater elasticity and higher biocompatibility. Ti purity is inversely proportional to the risk of allergic reactions [15, 17].

The selective laser melting process (SLM) is an unconventional manufacturing technology for customized substructure and bridges, as part of the Additive Manufacturing (AM). SLM manufacturing uses a solid laser that scans each metal powder layer. In the past years, SLM equipment was successfully used to manufacture the metallic CoCr substructure for fixed dental restoration (dental crowns and bridges) [18]. The technological novelty of this study is given by the use of pure Ti (99.5%) for the SLM manufacturing of metal-ceramic or metal-composite crowns. Unlike other studies that have analyzed FEA crowns on CoCr metal frame [19, 20, 21], the current study shows the effects of occlusal trauma in pure Ti prosthetic restorations. It also presents the SLM

manufacturing of the substructure which was CAD designed and processed by SLM from pure Ti powder.

The objective of this research study was to develop FEA mathematical models, with a high degree of fidelity in showing the anatomical dimensions of the natural tooth and the metal-ceramic or metal-composite crowns. The study evaluated the effect of the occlusal tensions by comparing the occlusal tension distribution in the entire right mandibular second premolar (4.5), when covered with a Ti-Ceramic and Ti-Composite crown.

2. Materials and Methods

2.1. Material selection

In this study, two types of dental crowns were developed as follows: a metal-ceramic restoration where a ceramic covering encases the Ti substructure (namely Ti-Ceramic) and a metal-composite restoration where composite also covers the Ti composite substructure (namely Ti-Composite).

The first veneering material selected is Titankeramik (VITA Zahnfabrik, Germany), an ultra-low fusing ceramic recommended for titanium substructures [22]. The second veneering material is Estenia (Kuraray, Japan), a hybrid composite [23]. This composite contains 8% urethane tetramethacrylate (UTMA) and hydrophobic dimethacrylate, 92% colloidal silica spheres with 16 wt% superfine microfillers (0.02 μm) and 76 wt% glass fillers (1.5- 2 μm) [23, 24]. The elasticity of this material is similar to that of the dentin, which makes it recommendable for use in dentistry [25].

The material used for cores is an especially gas-atomized Ti powder named TILOP45 (Osaka Titanium Technologies, Japan). This powder has a medium 45 μm particle diameter, the melting point around 1670 $^{\circ}\text{C}$, 4.53 g / cm³ density and it can be included in the category of pure Ti Grade I (because of 99.5% Ti). In comparison with the CoCr alloy, which has a density of 8.8 g / cm³ and a 200 GPa elasticity modulus, Ti has its physical characteristics halved, being slightly more elastic (details in Table 2). Besides high biocompatibility, Ti has Young's elasticity modulus similar to that of the gold alloy [26]. The physico-mechanical properties of all these biological materials are represented in Table 2.

2.2. Solid modelling of 3D reconstructions

In this study, we used CBCT images of a 26-year old clinically healthy female patient who volunteered in order for us to reconstruct 3D models. The cone beam computed tomography (CBCT) images were taken with a Promax scanner (Planmeca, Finland). The following scan parameters were used: 88 kV, 7 mA, 401 slices, 0.2 mm layer thickness, 10.6 cm x 10.6 cm field of view and an exposure time of 12 s. These CBCT images were imported in the MIMICS 13 software (Materialise, Belgium) where 3D masks were obtained for the cortical bone of the jaw, the dentin, the pulp and the enamel of the right lower

premolar (premolar 4.5), respectively. To reduce the size of the 3D models, the mandible was sectioned in the area related to the premolar 4.5 (Fig. 1). Thus, the cortical bone, the tooth consisting of dentin, pulp and enamel were exported in the format.STL to the CreoParametric software (Parametric Technology Corporation, USA). The periodontal ligament (PDL) was designed with this software by keeping a constant thickness of 0.25 mm and by copying the morphology of the root of the premolar 4.5 [14]. To render a model as closely as possible to a real tooth, the crown was designed as to copy the coronary morphology, while the metallic substructure was designed with a thickness of 0.5 mm, corresponding to a preparation with shoulder [27].

The first complex is the natural one and consists of enamel, dentin, pulp, PDL, cortical and trabecular bones and it is further referred to as "natural premolar". Fig. 1a shows all the seven designed parts that make up the prosthetic restoration which is composed of: the Ti substructure, the physiognomic component, the dentin, PDL, the pulp, and the cortical and trabecular bones. These parts were exported in .STEP format towards the ANSYS 16.0 WORKBENCH software (ANSYS Inc., USA). The luting agent layer was not considered a separate model due to its limited thickness and characteristics that are similar to dentin [14].

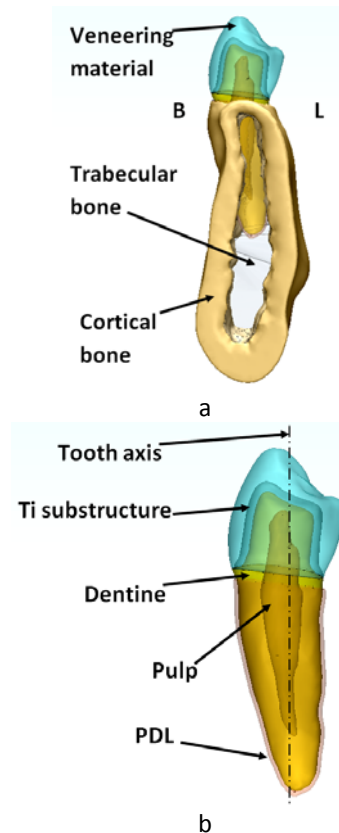


Fig. 1. a) Dental tissues and fixed dental restoration (distal view); The vertical axis of the premolar presents the loading direction of compressive force; Sides: B = buccal, L = Lingual; b) Natural premolar 4.5

2.3. FE analysis

In order to identify the effects of occlusal trauma on the dental tissues and on the Ti-Ceramic or Ti-Composite crowns, we applied compressive forces of between 67 and 454N. In adult women, a mastication force of 67 N is considered normal for the premolar 4.5 [28, 29], while the 454 N force can cause trauma and is associated with people with bruxism [19, 28]. Thus, in the current study six cases with the conditions from Table 1 were simulated. In Case 1 and 2, the direction of forces was parallel to the premolar axis (Fig. 1) and the contact areas were: buccal cusp tip, distal and mesial triangular fossa, respectively (Fig. 2a). The difference between the two cases is given by the fact that in Case 1 a load of 67N was exerted while in Case 2 the load was increased to 454N. In Case 3, a force of 135N was applied at an angle of 45° on the tip of the vestibular cusp, the contact area being that from Fig. 2b. In the same contact area Case 4 was simulated, and the difference was given by the direction of the force that was parallel to the main axis of the tooth (Fig. 2c). In Case 5 a load of 135N was applied on buccal triangular ridge (Fig. 2d), and in the last case (Case 6) the load was increased to 454 N. The direction of the force was oblique, being applied in the same area in both cases. All the contact areas were small in order to present mastication as realistically as possible, as was shown in previous studies [30].

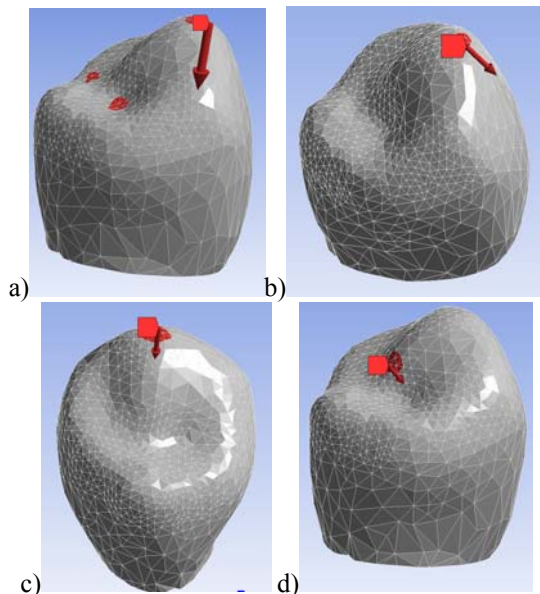


Fig. 2. Loading conditions for premolar 4.5, contact areas and force direction: a) Case 1 and Case 2, b) Case 3, c) Case 4, d) Case 5 and Case 6

Table 1. Loading conditions in lower premolar 4.5 for FE analyses

Case number	Load (N)	Loading positions and directions
Case 1	67	Parallel to long axis of the tooth in buccal cusp tip and distal respectively mesial triangular fossa
Case 2	454	Parallel to long axis of the tooth in buccal cusp tip and distal respectively mesial triangular fossa
Case 3	135	At a 45° oblique angle to the tooth axis in buccal cusp tip
Case 4	135	Parallel to long axis of the tooth in buccal cusp tip
Case 5	135	At a 45° oblique angle to the tooth axis in buccal triangular ridge
Case 6	454	At a 45° oblique angle to the tooth axis in buccal triangular ridge

The compressive force was uniformly distributed in the aforementioned occlusal contact areas and the von Mises equivalent stress data was analyzed. Boundary constraints were applied to the medial and distal cut surfaces of the mandible section following indications provided by [30, 31]: the medial nodes were restrained in x-axis translation (linguo-buccally), while the distal nodes were restrained both in the y- and z-axes (supero-inferiorly and mesio-distally).

In the ANSYS software, each model was assigned the appropriate physical characteristics, as shown in Table 2 (Young's modulus, Poisson's ratio, density). The materials were considered homogeneous and isotropic.

Initially the classical FEA method of simulation in ANSYS was used, but we identified major problems both in making the models discrete and in the subsequent transfer of the tensions between models, generating the geometrical concentrators of tensions. These tensions of the concentrators appear locally, in very small areas with high values of tension. Given these observations, the parameterization of all models in this entire dental complex followed using CAD methods. The finite element models were obtained by dividing them into 93,401 tetrahedral solid elements connected in 165,669 nodes.

Table 2. Elastic properties of isotropic materials

Material	Young Modulus [GPa]	Poisson's Ratio	Density [g/cm ³]	Compressive strength [MPa]	References
Ceramic Titankeramik	65	0.2	2.45	Above 300	[32]
Composite Estenia	22	0.27	2.50	Above 300	[24]
Titanium Grade J*	100	0.35	4.50	340-410	[33]
Dentine	18.6	0.311	1.486	275-300	[30]
Enamel	84.1	0.3	2.84	Up to 384	[30]
PDL	0.0689	0.45	1.06	-	[30]
Pulp	0.003	0.45	1.0	-	[34]
Trabecular bone	1.47	0.3	0.9	0.15-14	[35]
Cortical bone	14.7	0.3	1.74	Up to 212	[35]

* These physical-mechanical characteristics were obtained on standard samples manufactured by SLM process

2.4. Additive Manufacturing

For manufacturing the substructure from pure Ti the SLM REALIZER 250 (SLM Solutions GmbH, Germany) equipment was used. The system uses selective laser melting technology and could manufacture three-dimensional metal parts by fusing fine metallic powders together slice by slice, under a protective high-purity argon atmosphere. This technology utilizes a solid-state laser type Nd:YAG (neodymium-doped yttrium aluminum garnet $\text{Nd}^{3+}:\text{Y}_3\text{Al}_5\text{O}_{12}$) while the maximum power of laser beam is 200 W. The properties of Nd:YAG solid laser are as follows: 1064 nm emission wavelength in infrared spectrum, 230 μs duration of fluorescence, none birefringence (only thermally induced), 10–14 W/(m²*K) thermal conductivity and $7\text{--}8 \times 10^{-6}/\text{K}$ thermal expansion coefficient. In previously carried out studies, the optimal process parameters for the proper physico-mechanical characteristics of Ti were obtained by using 120 W laser power, 500 mm/s scanning speed of laser and 50 μm layer thickness of powder [33]. The energy input of each hatch scanning was calculated at 43.63 J/mm³ (according to [29]). These parameters were set to scan the hatch, and Table 1. shows the physical characteristics obtained on standard specimens in these conditions in the SLM process. To achieve a proper quality surface and a reduction in the time and in the post-processing costs, previously carried out studies showed that the optimum parameters for scanning the outer boundary of parts are:

133 W laser power and 344 mm/s scanning speed of laser [36]. With these processing parameters, 10 Ti-capets were manufactured via SLM and were covered in ceramic and composite afterwards.

3. Results

The results of the six cases are shown in Fig. 3-8, and the von Mises equivalent stress was analyzed. In order to identify the tensions more easily, Fig. 3-8 have the same scale of values. These scales were used to determine the limit values for the dentin resistance to compression (up to 300 MPa) and for those of the cortical bone (maximum 212 MPa). Tables 3 and 4 show the maximum values of equivalent von Mises stress and of the total deformation recorded in each case.

In all the simulated conditions, it was demonstrated that there were no tensions in the cortical bone close to its limit of breaking. In the current study, the tensions in the cortical bone were between 10-168 MPa. This can be explained by the fact that tensions were distributed up to the apex. In nearly every case simulated by FEA, the contact areas of the Ti-Ceramic and Ti-Composite crowns were loaded with similar values of tensions, but slightly higher than those in the natural enamel. In all the six cases studied by FEA it was found that PDL absorbed tensions and distributed them almost entirely in the cortical bone.

Table 3. Maximum equivalent von Mises stress (MPa)

	Case 1	Case 2	Case 3	Case 4	Case 5	Case 6
Natural premolar	39.68	268.88	280.69	149.36	218.45	734.65
Ti-Ceramic restoration	45.70	309.71	299.18	142.33	238.78	803.00
Ti-Composite restoration	45.22	306.47	298.91	146.14	221.48	744.83

Table 4. Total deformation values (mm)

	Case 1	Case 2	Case 3	Case 4	Case 5	Case 6
Natural premolar	0.003	0.021	0.064	0.013	0.048	0.161
Ti-Ceramic restoration	0.003	0.022	0.066	0.014	0.048	0.163
Ti-Composite restoration	0.004	0.030	0.078	0.018	0.051	0.174

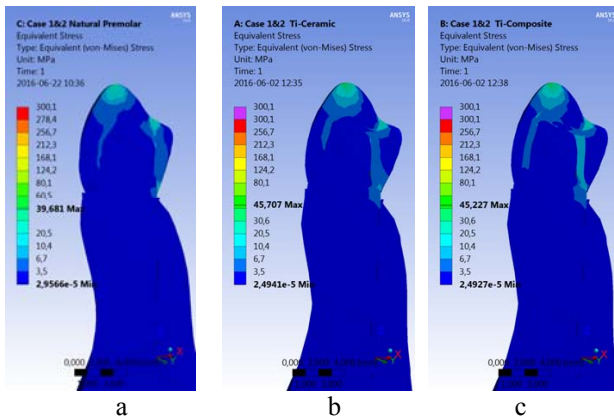


Fig. 3. Distribution of the von Mises equivalent stress in Case 1: a) Natural premolar, b) Ti-Ceramic and c) Ti-Composite

The first case shown in Fig. 3 simulates maximum functional intercuspation in three points of the premolar 4.5. The total load of 67 N was applied parallelly to the main axis of the tooth. In these anatomical conditions, low tension (below 6.7 MPa) was distributed in the dentin of the natural premolar, while the highest values were recorded in the enamel (fig. 3a).

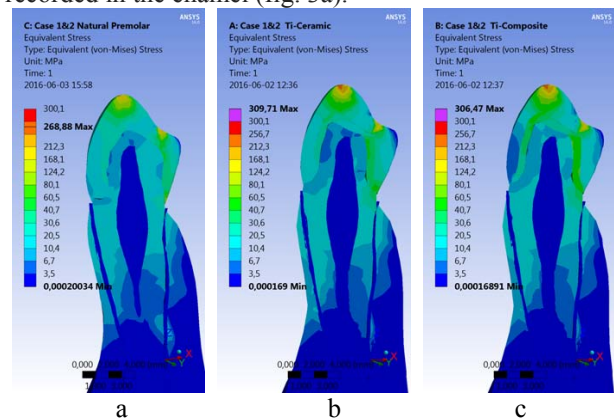


Fig. 4. Distribution of the von Mises equivalent stress in Case 2: a) Natural premolar, b) Ti-Ceramic and c) Ti-Composite

The second case (Fig. 4) shows the results after a mastication load of 454 N was applied in the three areas shown in Fig. 2a. In this case the maximum tension could be noticed to have occurred in the Ti-Ceramic crown (309.71MPa). In the metallic substructure of the Ti-Composite crown, tensions of 30-80 MPa were present, whereas the Ti-Ceramic crown was loaded with lower tensions. Thus, the Ti-Ceramic crown distributes lower tension in the dentin. The ceramic crown was found loaded in almost all its volume, behaving as the natural enamel (Fig. 4 a and b). By contrast, the composite crown distributes tension only partially, leaving areas loaded below 10 MPa (buccal side). However, high tension values were recorded in the cervical third (approx. 80 MPa) in all these three cases.

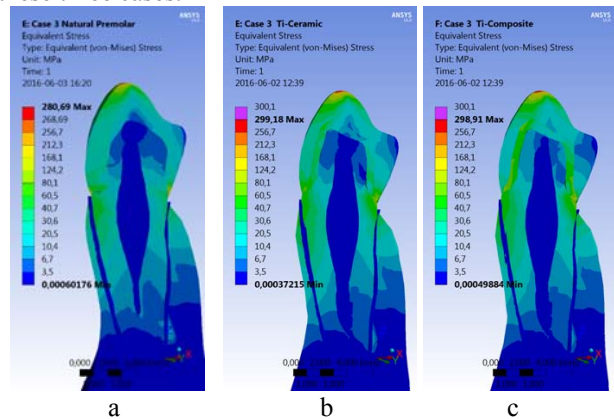


Fig. 5. Distribution of the von Mises equivalent stress in Case 3: a) Natural premolar, b) Ti-Ceramic and c) Ti-Composite

Fig. 5 shows Case 3 where high tension was found in the cervical third and the periodontal area. Because of the change in the force direction, the metallic substructure of the Ti-Composite crown was loaded with higher tensions (up to 168 MPa) both in the margin of the shoulder and in the apical area (Fig. 5c). By contrast, the substructure of Ti-Ceramic crown was loaded with tensions between 40-124 MPa; the highest ones, though, were located in the cervical third. The Ti-Ceramic crown behaved similarly to natural tooth tissues.

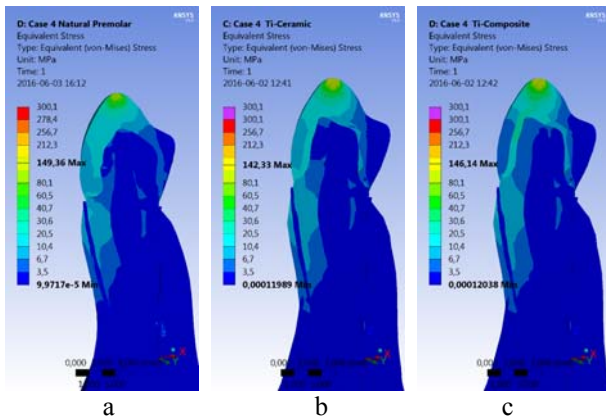


Fig. 6. Distribution of the von Mises equivalent stress in Case 4: a) Natural premolar, b) Ti-Ceramic and c) Ti-Composite

Case 4 is shown in Fig. 6, where a force of 135 N was applied parallelly to the tooth axis in the contact area (detail in Table 1). The results of this simulation showed similar distribution of tensions in the natural premolar and in the Ti-Ceramic crown. Due to the elastic properties of the composite material, the metallic substructure of the Ti-Composite crown became locally loaded, which was not favorable for good functioning.

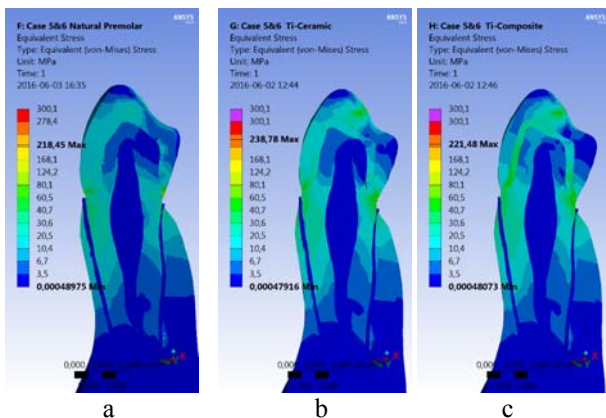


Fig. 7. Distribution of the von Mises equivalent stress in Case 5: a) Natural premolar, b) Ti-Ceramic and c) Ti-Composite

Case 5, shown in Fig. 7, is the result of the application of para-axial force of 135 N in the area shown in Fig. 2d. Accumulations of tensions were found in the cervical third and in the PDL (periodontal ligament). The metallic substructure of the Ti-Ceramic crown takes on some of the tension and partly amortizes it, behaving like the natural tooth.

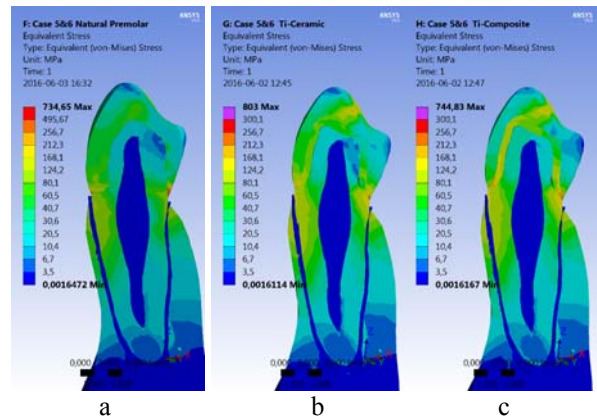


Fig. 8. Distribution of the von Mises equivalent stress in Case 6: a) Natural premolar, b) Ti-Ceramic and c) Ti-Composite

Fig. 8 shows a possibly pathologic loading (Case 6, Table 1). The maximum occlusal load of 454 N was distributed in the contact points and we can assume that in occlusal trauma, breaking can occur in the physiognomic material or in the Titankeramik ceramic and Estenia composite, respectively. In the Ti substructure of the two prosthetic restorations, tension below the compressive strength of Ti and up to 300 MPa was distributed (Fig. 9). Furthermore, both the Ti-Ceramic crown and the Ti-Composite crown distribute tensions below 212 MPa in the dentin. Basically, even in this extreme case, the Ti substructure takes on some of the tensions and partly amortizes it due to its specific elasticity characteristics (as shown in Table 2). No major tension with impact on the dentin was distributed in it, the dentin resisting a compression of over 275 MPa. Moreover, the situations shown in Figures 8b and 8c indicate that in the cortical bone, tension does not exceed 168 MPa or 124 MPa, when one of the two restorations presented before is used or in the case of the healthy natural premolar, respectively. Even in these conditions, higher tensions were recorded in the cervical third.

The total deformations in the 6 analyzed conditions had close values in the natural premolar and in the Ti-Ceramic crown. The total deformations were between 0.003-0.174 mm, and the Ti-Composite crown was found with slightly higher values compared to the other cases. Because of the much more different elasticity properties of the composite, the crowns covered in this material suffered more deformations, which can be seen in Fig. 10.

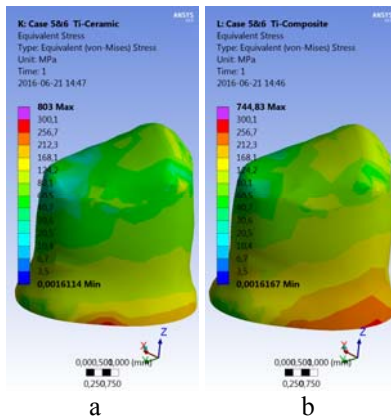


Fig. 9. Distribution of the von Mises equivalent stress in Ti substructure, loading conditions of Case 6: a) Ti-Ceramic, b) Ti-Composite

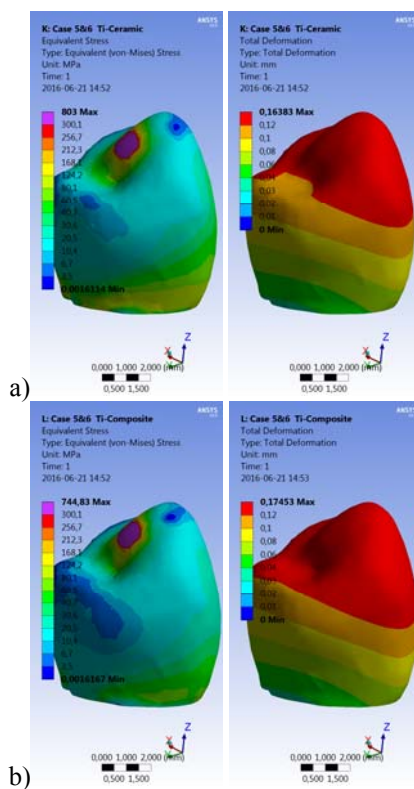


Fig. 10 Distribution of the von Mises equivalent stress and total deformation in the veneering material, loading conditions of Case 6: a) Ti-Ceramic, b) Ti-Composite

The Ti substructure manufacturing was achieved using SLM equipment with the process parameters given above. No incidents were recorded during the manufacturing by SLM, and the process took place under normal conditions and resulted in the substructure shown in Fig. 11. By using the best parameters for scanning the outer boundary, the surfaces of the Ti substructure had a roughness defined by R_a of $4.1 \mu\text{m}$ (R_a - arithmetic average of absolute values). After manufacturing, the substructure was sandblasted with aluminum oxide with

110-150 μm grit and a pressure of 2-3 bar. Finally, on the outer surface the Ti substructure (Fig.11) was covered with Titankeramik and Estenia composite.



Fig. 11. Dental Ti substructure manufactured by SLM

4. Discussions

The use of FEA methods allows testing various physiological scenarios by applying mastication loads on the virtual model of the natural premolar and of the dental crowns, without affecting the integrity of the original specimen. In the study, six different scenarios were created. We used two analyses based on the existing contact areas during the maximum intercuspation, two analyses with punctiform force and two analyses that simulate the presence of interference.

The tension produced during mastication was transmitted from the tooth surface to its support structures (e.g. PDL and the alveolar bone), which was reported by other authors too [3, 37]. In order to analyze a real case more accurately, the crown was designed with a chamfer shoulder as in the most common clinical situations.

Dentists often face this situation because preparations are known to be difficult to achieve, especially in the lingual surfaces of the lower teeth [38]. Clinical studies show that restorations fail because of bacterial infiltration or mechanical action [39, 40].

The veneering material significantly affected tension concentration, which was reported by many authors [15]. Titankeramik ceramic has a 65 GPa Young modulus (closer to 84 GPa of the natural enamel), while the Estenia composite is more elastic and has a 22 GPa Young modulus (closer to 18 GPa of the natural dentin). The low elasticity modulus of the Ti parts manufactured by SLM (100 GPa), led to loading the Ti substructure and to distributing this load in the dentin with a lower intensity, which was found in all the 6 FEA investigated cases. It was also found that the composite material took on and distributed the tension almost entirely in the Ti substructure, leading to slightly higher tension in the dentin in comparison with the behavior of the natural premolar. Ti-Ceramic prosthetic restoration amortized some of the tensions in the dentin and distributed approximately the same tension as the natural enamel. These aspects can also be observed in Fig. 9, which shows the distribution of tensions in the Ti substructure for Case 6. In this case we identified large areas with tensions between 168-256 MPa, in the Ti-Composite substructure (Fig. 9b), and by the same scale, the substructure covered in ceramic was loaded with similar tensions on smaller areas.

Comparable behavior regarding the distribution of tension in the natural premolar and the Ti-Ceramic restoration results from the fact that the morphology of the crown (outer boundary) has the same shape as the enamel, but in practice the accuracy of the morphology is difficult to achieve because it involves a high degree of specialization on behalf of the dental technician. The Ti substructure designed in this study had a thickness of 0.5 mm and was applied to a preparation with shoulder. Following research with FEA methods, the Ti substructure was found to be loaded without reaching its breaking limit even in Cases 2 and 6, in which loads of 454 N were applied. In comparison with an substructure fabricated from CoCrWMo alloy with the same volume, the Ti substructure had a lower weight by 46%.

FEA studies also showed the fact that the ceramic material distributed tension evenly throughout its entire volume, while the composite material took on the local tension and partly distributed it in its volume, increasing the Ti substructure loading. This type of reaction can be explained by the fact that ceramic materials are stiffer than the composite ones.

In Cases 1 and 2 the maximum occlusal load was evenly distributed in the points of coronary contact. One can hypothesize that they may contribute to the increase in the local structural resistance of the tooth, thus directing a part of the load applied in the central part of the dental crown and reducing the tension from the crown.

Case 3 simulated the effects of oblique loads with higher levels of von Mises equivalent stress (299 MPa) as compared to Case 4, in which the same intensity load was applied but the direction was parallel to the axis of the tooth. Moreover, in Case 3 after applying an oblique load, the distribution of the highest tension was found in the cervical third and in the contact area, respectively.

Cases 5 and 6 constitute two scenarios that simulate interferences in the movements of laterality. The applied load had the same direction but a different magnitude. It was found that, regardless of the intensity of the load, tension was located in the cervical third, in the support periodontium and in the cortical bone.

These findings may be useful for a better understanding of the reaction of the periodontal ligament to the mastication load. Furthermore, they can be useful for the biomechanical quantification of the impact of different occlusal cases on dispersing occlusal forces. Thus, using finite element method we are able to load several options, namely: change of load conditions, change of limit conditions, of their way of application upon the virtual model, out of which the optimal choice for the structure of the advanced material can be selected [41].

The main advantages of SLM fabrication are: that it could provide dental prosthetic restorations more quickly, less expensively, without compromising their quality in comparison with restorations prepared by casting and milling techniques [18, 36]. Considering its specific characteristics (the low density and the presence of Young modulus), conclusion can be drawn that Ti is a good alternative to CoCr alloys and it is, therefore, recommended for use in metallo-ceramic restorations.

Moreover, pure Ti could be used for metal-sensitive individuals as cases of Ti-hypersensitivity reactions were rarely reported [15, 42].

5. Conclusions

All these studies by FEA methods show the importance of the elasticity features of the materials used in dental prosthetics, especially for dental reconstructions made from Ti metal frames covered in ceramic or composite materials.

Alongside with the reduction in the elasticity Young modulus of the substructure material that covers the Ti corresponding prosthetic restorations, the metallic substructure was loaded during mastication with high tensions that were then distributed in the preparation. Thus, the Estenia composite, which has a Young modulus of 22 GPa, took on and distributed tension in the Ti substructure and in the dentin, respectively, which was higher compared to Titaneramik ceramic (Young modulus of 65 GPa).

The enamel and the Ti-Ceramic crown behaved in a comparable way and distributed similar tension in the dentin. The highest tension was located in the contact points and in the cervical third.

Total deformations in the 6 analyzed conditions have comparable values in the natural premolar and in the Ti-Ceramic crown. Pure Ti has lower density and rigidity than the CoCr alloy, which makes it suitable as support for dental prosthetic restorations.

The current research describes in detail the main stages of the design and manufacturing of the metal frames which were customized and processed by SLM and in which pure Ti powder was used. AM technologies, particularly the SLM process, can be effective in manufacturing related Ti frames in prosthetic restorations. The results of the FEA studies can be used in dental prosthetics to achieve the correct therapeutic procedure, especially for treating patients with allergic reactions to metals.

Acknowledgements

This research was supported by the AM-CIR project, PN-II-RU-TE-2014-4-1157, no. 37/01.10.2015 financed from the UEFISCDI by the Romanian Government.

References

- [1] D. Palamara, J. E. A. Palamara, M. J. Tyas et al Dent. Mater. **16**, 412 (2000).
- [2] B. Dejak, A. Młotkowski, M. Romanowicz. J. Prosthet. Dent. **90**, 591 (2003).
- [3] C. Bică, K. Martha, D. Cerghizan, M. Suciuc, B. Petcu, D. Bică, D. Eșian, J. Optoelectron. Adv. M. **17**(11-12), 1756 (2015).
- [4] G. T. Schwartz. Am. J. Phys. Anthropol. **111**(2) 221 (2000).

- [5] I. A. Poiate, A. B. de Vasconcellos, R. B. de Santana, E. Poiate, *J. Periodontol.* **80**(11), 1859 (2009).
- [6] K.. M. Hiimae. In: *Food Acquisition and Processing in Primates*. Chivers DJ, Wood BA, Bilsborough A 1984. eds. New York: Plenum Press. p 257-282.
- [7] B. Hojjatie, K. J. Anusavice. *J Biomech.* **23**(11), 1157 (1990).
- [8] D. Palamara, J. E. A. Palamara, M. J. Tyas, H. H. Messer. *Dent. Mater.* **16**(6),412 (2000).
- [9] P. Kamposiora, G. Papavasiliou, S.C. Bayne, D. A. Felton. *J. Prosthet. Dent.* **71**(15), 435 (1995).
- [10] K. A. Proos, M. V. Swain, J. Ironside, G. P. Steven. *Int. Prosthodont.* **16**(4):442 (2003).
- [11] K. A. Proos, M. V. Swain, J. Ironside, G. P. Steven. *Int. J. Prosthodont.* **16**(1), 82 (2003).
- [12] K. A. Proos, M. V. Swain, J. Ironside, G. P. Steven. *Int. J. Prosthodont.* **15**(4), 404 (2002).
- [13] K. A. Proos, M. V. Swain, J. Ironside, G. P. Steven. *Int. J. Prosthodont.* **16**(5):474 (2003).
- [14] I. A. Poiate, A. B. de Vasconcellos, R. B. de Santana, E. Poiate. *J. Periodontol.* **80**(11), 1859 (2009).
- [15] C. G. Dumitras, R. Cerna, T. Stamate, M. Vardavoulis, J. Optoelectron. *Adv. M.* **16**(11-12), 1447 (2014).
- [16] G. Fu, F. Deng, L. Wang, *Ren Dent Traumatol.* **26**(1), 64 (2010).
- [17] B. S. Maluckov, *Optoelectron. Adv. Mat.* **8**(5-6), 545 (2014).
- [18] T. Koutsoukis, S. Zinelis, G. Eliades, K. Al-Wazzan, M. A. Rifaiy, Y. S. Al Jabbari. *J Prosthodont* **24**(4), 303 (2015).
- [19] R. Prabhu, G. Prabhu, E. Baskaran, E. M. Arumugam *J. Indian Prosthodont. Soc.* **16**(2), 193 (2016).
- [20] Z. Huang, L. Zhang, J. Zhu, X. Zhang. *J. Prosthet. Dent.* **113**(6), 623 (2015).
- [21] E. Tamac, S. Toksavul, M. Toman. *J. Prosthet Dent.* **112**(4), 909 (2014).
- [22] V.Z. Vásquez, M. Ozcan, E.T. Kimpara. *Dent Mater.* **25**(2), 221 (2009).
- [23] M. M. Gresnigt, W. Kalk, M. Ozcan. *J. Adhes. Dent.* **15**(2), 181 (2013).
- [24] Akikazu Shinya, Daichiro Yokoyama. *Finite Element Analysis for Dental Prosthetic Design, Finite Element Analysis*, David Moratal (Ed.), InTech, DOI: 10.5772/10006. Available from: <http://www.intechopen.com/books/finite-element-analysis/finite-element-analysis-for-dental-prosthetic-design>. (2010).
- [25] R. de Castro Albuquerque, L.T. Polleto, R.H. Fontana, C.A. Cimini. *J Oral Rehabil.* **30**(9), 936 (2003).
- [26] N. De Jager, M. de Kler, J.M. van der Zel. *Dent Mater.* **22**(3), 234 (2006).
- [27] J. W. Oh, K. Y. Song, S. G. Ahn, J. M. Park, M. H. Lee, J. M. Seo. *J Adv Prosthodont.* **7**(5), 349 (2015).
- [28] Y. Duan, J. A. Griggs. *J Dent.* **43**(6), 742 (2015).
- [29] P. Magne, U. C. Belser. *Int. J. Periodontics Restorative Dent.* **22**(5), 425 (2002).
- [30] S. Benazzi, I. R. Grosse, G. Gruppioni, G. W. Weber, O. Kullmer. *Clin. Oral Investig.* **18**(2), 369 (2014).
- [31] S. Benazzi, O. Kullmer, I. Grosse, G. Weber. *Am. J. Phys. Anthropol.* **147**(1), 128 (2012).
- [32] N. Suansuwan, M. V. Swain. *J Oral Rehabil.* **28**(2), 133 (2001).
- [33] C. S. Cosma, N. Balc, D. Leordean, M. Moldovan, M. Dudescu. *AJME*, **13**, 2 (2015).
- [34] M. S Guler, C. Guler, F. Cakici, E. B. Cakici, S. Sen, Niger. *J Clin Pract.* **19**(1), 30 (2016).
- [35] Y. Zhao, W. Wang, H. Xin, S. Zang, Z. Zhang, Y. Wu. *Med Biol Eng Comput.* **51**(9), 991 (2013).
- [36] N. Bâlc, S.C. Cosma, J. Kessler, V. Mager. *Research on improving the outer surface quality of the parts made by SLM*, MTeM Conference, Cluj-Napoca, 2015.
- [37] K. Bica, D. Martha, T. Marcu, P. Berce, N. Balc. *Rapid Prototyping Journal* **21**(1), 98 (2015).
- [38] C. C. Begazo, J. M. Van Der Zel, M. A. J. Waas, A. J. Feilzer. *Am. J. Dent.* **17**(6), 437 (2004).
- [39] Tao You, Qiman Wu, Yingjie Xu. *Optoelectron. Adv. Mat.* **9**(5-6), 709 (2015).
- [40] F. H. Van de Sande, N. J. Opdam, P. A. Rodolpho, M. B. Correa, F. F. Demarco, M. S. Cenci, *J. Dent. Res.* **92**(7 suppl), 78S (2013).
- [41] A. E. Stanciu, D. L. Cotoros, L. Cristea, M. Bartiz. *J. Optoelectron. Adv. M.* **17**(7-8), 1146 (2015).
- [42] M. M. Dicu, M. Ursu, C. Ungureanu, P. C. Dicu, S. Popescu. *J. Optoelectron. Adv. M.* **17**(11-12), 1816 (2015).

*Corresponding author: ispas.ana@umfcluj.ro